

Participation in the absolute gravity comparison with a compact cold atom gravimeter

Zhijie Fu (付志杰)^{1,2}, Qiyu Wang (王启宇)¹, Zhaoying Wang (王兆英)^{1,*}, Bin Wu (吴彬)², Bing Cheng (程冰)², and Qiang Lin (林强)^{2,**}

¹*Institute of Optics, Department of Physics, Zhejiang University, Hangzhou 310027, China*

²*Center for Optics and Optoelectronics Research, College of Science, Zhejiang University of Technology, Hangzhou 310023, China*

*Corresponding author: zhaoyingwang@zju.edu.cn; **corresponding author: qlin@zjut.edu.cn

Received October 27, 2018; accepted November 23, 2018; posted online December 28, 2018

The first Asia-Pacific Comparison of Absolute Gravimeters (APMP.M.G-K1) was organized by the National Institute of Metrology (NIM) of China from December 21, 2015 to March 25, 2016 in Changping, Beijing. Our compact cold atom gravimeter (CCAG) was transported from Hangzhou to Beijing with a long distance of about 1200 km to participate in this comparison. The CCAG is the only one, to the best of our knowledge, that is based on the principle of atom interferometry among all the instruments. Absolute gravity in the indicated three test sites has been measured as requested by the organizer. The sensitivity of our CCAG is estimated to be $90 \mu\text{Gal}/\sqrt{\text{Hz}}$, even when the measurements are carried out without any vibration isolation. Besides, the accuracy of this gravimeter has been evaluated to be about $19 \mu\text{Gal}$ by considering the significant system errors. Our results show a good agreement with the given reference value.

OCIS codes: 120.3180, 120.3940.

doi: 10.3788/COL201917.011204.

High-precision measurement of absolute gravity has a wide application in geophysics, geology, hydrology, volcanology, etc. Accurate gravity measurement of a several micro-gal (μGal)-level could reveal subtle changes in geological activities. For example, gravity values increasing by $4 \mu\text{Gal}$ can indicate 1 m elevation rising of volcanic lava level^[1]: scientists make this conclusion after long-time precise gravity monitoring around the Kilauea Volcano. Besides, volcanic activities may be predicted by continuous absolute gravity measurements. Scientists found that quick gravity decreasing and recovering of about $10 \mu\text{Gal}$ occurred before most volcanic eruption events^[2]. On the other hand, accurate absolute gravity measurements also play an important role in hydrological observations. Recent reports indicate that the changes of local water storage are strongly correlated to local gravity variance. When the water storage level rises by 100 mm, the gravity value will increase about $4 \mu\text{Gal}$ ^[3].

The accuracy of an absolute gravimeter (AG) is hardly to be verified by itself, because the local absolute gravity value is always changing with time and position. The only way to verify its accuracy is to make comparisons with other high-precision AGs, such as bilateral comparison^[4-6], regional comparison^[7-9], and international comparison^[10,11]. Since a free-falling corner cube (FFCC)-type AG is based on different working principles compared with atom interferometry (AI)-type AG, bilateral comparison between them will be beneficial for both instruments. For example, the research group from the National Institute of Metrology (NIM) of China demonstrated their cold atom AG (CAAG), showing an agreement of $-0.2(6.3) \mu\text{Gal}$ compared with an FG5X^[12]. The International Comparison of Absolute

Gravimeters (ICAG) is the most authoritative and convincing gravimeter comparison. The eighth ICAG was held in 2009, which was the first ICAG organized as a key comparison^[10]. Most of the participating AGs are the FG5 type, a state-of-the-art commercial FFCC-type AG^[13,14]. The FG5-type AG could reach the highest accuracy of about $2 \mu\text{Gal}$, which has been widely applied on many occasions of accurate absolute gravity measurements. A CAAG from LNE-SYRTE (France, type CAG-01)^[15] had participated in this comparison. It was the first successful application of the CAAG in the field of gravity metrology. The final measured results of CAG-01 were $-1.6(3.6) \mu\text{Gal}$ compared with the key comparison reference values. The results indicate that the CAAG has reached the corresponding accuracy compared with FG5. CAG-01 also participated in regional or international comparisons, such as the European Comparison of Absolute Gravimeters (ECAG) 2011 and ICAG2013^[11]. In 2017, the 10th ICAG was held by NIM of China in Beijing, and six CAAGs participated in the comparison. The related reports will be issued by the organizer.

Since the advent of AI in 1990s, applications based on the cold atom have made tremendous progress^[16-19]. AI has wide applications in both the fields of fundamental physics and applied physics, such as the measurement of fundamental physics constants^[20-22], the tests of the general relativity^[23], the equivalence principle^[24], and the exploration for gravitational waves^[25]. The test of the equivalence principle at 10^{-8} level has been accomplished by the Wuhan Institute of Physics and Mathematics with the method of dual-species double-diffraction Raman atom interference^[26]. AI-type AGs have great advantages,

such as excellent stability, high repetition rate, and high accuracy and sensitivity, for example, a sensitivity of $4.2 \mu\text{Gal}/\sqrt{\text{Hz}}$ in the Huazhong University of Science and Technology (HUST)^[27]. Compared with other accurate AGs, the free-fall test mass of CAAG is the cold atom rather than macroscopic objects, such as a corner cube. It makes the CAAG more suitable for continuous absolute gravity monitoring and has better immunity with respect to changes of vibration noise^[28]. Since the development of integrated electronic technology and integrated optical devices, mobile CAAG has made a great progress^[29,30]. In recent years, the CAAG has already achieved field applications^[31]. For example, in 2013, the compact gravimetric atom interferometer (GAIN) from Heidelberg University achieved mobile measurement of absolute gravity with a sensitivity of $30 \mu\text{Gal}/\sqrt{\text{Hz}}$ ^[32]. Another gravity measurement in an elevator has been reported with a sensitivity of $42 \mu\text{Gal}/\sqrt{\text{Hz}}$ ^[33]. It is promising for CAAG to surpass the other state-of-the-art AGs.

Recently, we accomplished a compact CAAG and transported by an air-cushioned and air-conditioned truck to the Changping campus of NIM, China to participate in the first Asia-Pacific Comparison of Absolute Gravimeters (APMP.M.G-K1). In this comparison, the absolute gravity of three sites at different locations was measured as requested by the organizer, with a measuring time of 12 h for each site. The most significant system errors were evaluated so that the total instrument uncertainty is estimated to be $19 \mu\text{Gal}$.

The principle of the atomic gravimeter has been discussed in great detail in Ref. [34]. Our inertial sensor is a Mach-Zehnder-type interferometer. The separation and reflection of the atomic matter waves are realized by inducing a two-photon Raman transition. The transitions mainly occurred within two ground states of hyperfine levels of ^{87}Rb , that is $5^2\text{S}_{1/2}$, $F = 2$ and $5^2\text{S}_{1/2}$, $F = 1$. Two counter-propagating Raman laser beams with a wave vector of \vec{k}_1 and \vec{k}_2 , respectively act on the atoms with a pulse sequence of $\pi/2 - \pi - \pi/2$. Suppose all the atoms are in the initial state of $5^2\text{S}_{1/2}$, $F = 2$, and the first $\pi/2$ pulse separates the atoms into two states; about one-half is in the state of $5^2\text{S}_{1/2}$, $F = 2$ and another half is in the state of $5^2\text{S}_{1/2}$, $F = 1$. Then, the atoms fall freely in the gravitational field during the interrogation time T , and a π pulse is applied, which acts as a mirror, realizing the complete transition from the state of $5^2\text{S}_{1/2}$, $F = 2$ to the state of $5^2\text{S}_{1/2}$, $F = 1$, and vice versa. After another flight time T , the second $\pi/2$ pulse recombines the atomic wave packet, and then the atoms in two states interfere with each other. The transition probability P can be described as

$$P = [1 \pm \cos(\vec{k}_{\text{eff}} \cdot \vec{g} - \alpha)T^2]/2. \quad (1)$$

Here, $\vec{k}_{\text{eff}} = \vec{k}_1 - \vec{k}_2$ is the effective wave vector of Raman pulses, T is the time interval of two sequential Raman pulses, α is the frequency chirp rate of Raman lasers for compensating the Doppler shift due to gravitational field, and \vec{g} is the acceleration of gravity.

The experimental apparatus mainly consists of two parts: a mobile sensor system and a compact control system. The sensor system contains a two-dimensional (2D) and three-dimensional (3D) magneto-optical trap (MOT) with their accessory optics units and magnetic field coils. The control system includes an electronic control module and a compact laser system, which manipulates optical, electronic, and magnetic signals to the sensor system.

The schematic diagram of the sensor system is shown in Fig. 1. Its main parts include a 2D-MOT and a 3D-MOT vacuum chamber made by titanium alloy, which is non-magnetic and with high-strength. The detection region is under the 3D-MOT chamber by about 20 cm, and a fluorescence collecting system is also located there. Several collimators and magnetic field coils adhere to the chamber in appropriate places to provide laser beams and a magnetic field for the experiment. A magnetic shield, consisting of two layers of permalloy, covers the 3D-MOT chamber and detection region.

The compact laser system has been illustrated in detail in our previous paper^[20]. Two distributed feedback (DFB) laser diodes of 1560 nm provide all of the laser beams. One of them, namely the reference laser, is locked to a rubidium transition. Another one is the master laser, which is locked to the reference laser by the beat signal, power amplified by an erbium-doped fiber amplifier (EDFA), and frequency doubled in a periodically poled lithium niobate (PPLN) crystal. The master laser provides about 1 W laser output with the wavelength of 780 nm for the main optical path. The frequencies of repumping and Raman lasers are modulated by an electro-optic modulator (EOM) and controlled by a compact radio frequency (RF) box. The DFB lasers and frequency-locking module are integrated in a standard 19 in. cabinet. The remaining optical paths are integrated in an optical platform with dimensions of $900 \text{ mm} \times 520 \text{ mm} \times 130 \text{ mm}$, where the

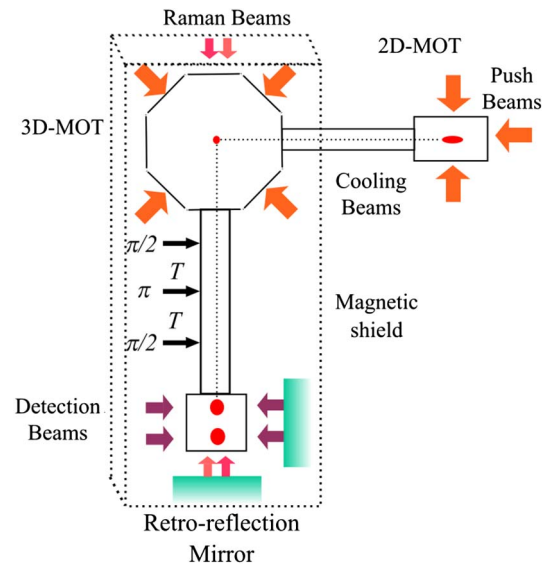


Fig. 1. Schematic diagram of the gravity sensor.

laser beams are coupled into the single-mode and polarization-stabilized fibers and sent to the sensor system.

The electronic control modules are well-organized in a self-designed aluminum shelf with a size of $113\text{ cm} \times 78\text{ cm} \times 150\text{ cm}$. Most of the modules are homemade, including a digital frequency hopping locking (DFHL) module, a direct digital synthesizer (DDS) module, three acousto-optic modulator (AOM) drivers, and a compact RF box. In addition, some commercial modules, such as the laser control and several power sources, are also applied. The picture of the CCAG in the test field is shown in Fig. 2.

Detailed experimental procedures will be described in this section. First of all, ^{87}Rb atoms are pre-cooled in a 2D-MOT and then pushed to a 3D-MOT via a differential tube by a push beam. In the 3D-MOT, about 10^9 atoms are loaded within 400 ms. In order to further lower the temperature of atoms, polarization gradient cooling (PGC) is carried out. Finally, the temperature of the cold atoms molasses is $5\text{ }\mu\text{K}$. After that, all of the optical and magnetic fields are turned off in order to let the atoms fall freely in the gravitational field. Then, two microwave π pulses resonating with two ground states of $|F=2, m_F=0\rangle$ and $|F=1, m_F=0\rangle$ of the ^{87}Rb atom act on the atoms in order to pick out the atoms in the state of $|F=2, m_F=0\rangle$, which is insensitive to the magnetic field. Next, a Raman π pulse acts on the atoms in order to obtain a narrow vertical velocity distribution in the state of $|F=1, m_F=0\rangle$. Then, about 1×10^5 atoms (in the state of $|F=2, m_F=0\rangle$) with a temperature of $2\text{ }\mu\text{K}$ of vertical velocity distribution are selected for the interference process. In the following, a sequence of Raman pulses ($\pi/2 - \pi - \pi/2$) induces the interference of the atoms in the two ground states. The duration of the Raman π pulse is $20\text{ }\mu\text{s}$.

Finally, a pair of counter-propagating detecting laser beams illuminates on the falling atoms. The fluorescence is collected by the fluorescence collecting system. We adopt a method of time of flight (TOF) to evaluate the number and the temperature of atoms. In order to reduce the influence brought by the fluctuation of the atom number, the normalized detection method was utilized.

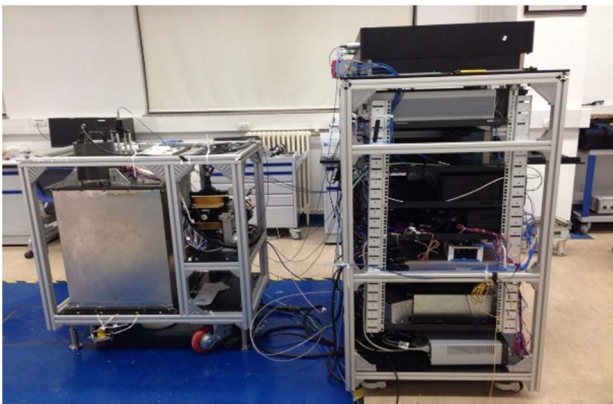


Fig. 2. Picture of the CCAG in the test field.

The flight time of atoms from 3D-MOT to the detection region is about 200 ms. With the loading time of 400 ms and a buffer time of 100 ms, the whole time of one experimental cycle was 700 ms; in other words, the repetitive rate was 1.4 Hz. With the sweep of the frequency chirp rate α , the fringe of atomic interference can be obtained, which is shown in Fig. 3.

After the comparison, we take a long-term gravity measurement in one comparison field. The continuous 36 h gravity data is shown in Fig. 4. The experimental data is consistent with the theoretical tidal model. The residuals of the experimental data and tidal model are within $20\text{ }\mu\text{Gal}$.

Figure 5 shows the Allan standard deviation of the residuals signals. The equivalent sensitivity at 1 s is $90\text{ }\mu\text{Gal}$. A resolution of $6.5\text{ }\mu\text{Gal}$ is obtained after an integration time of 200 s, and $4\text{ }\mu\text{Gal}$ is achieved within 1000 s integration time.

We transport our CCAG by an air-cushioned truck to participate in the APMP.M.G-K1, which is held in Beijing, as shown in Fig. 6. The truck is equipped with a vibration isolation and air-conditioner system. The CCAG was still in a good operating status after being transported about 1200 km from Hangzhou to Beijing.

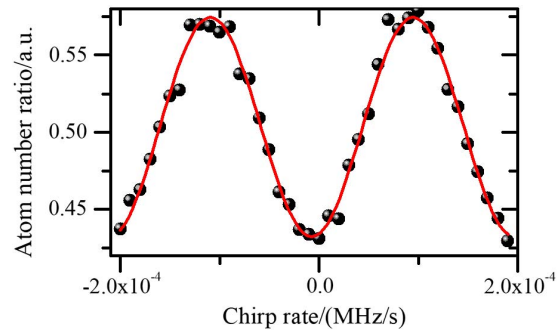


Fig. 3. Atomic interference fringe for $T = 70\text{ ms}$.

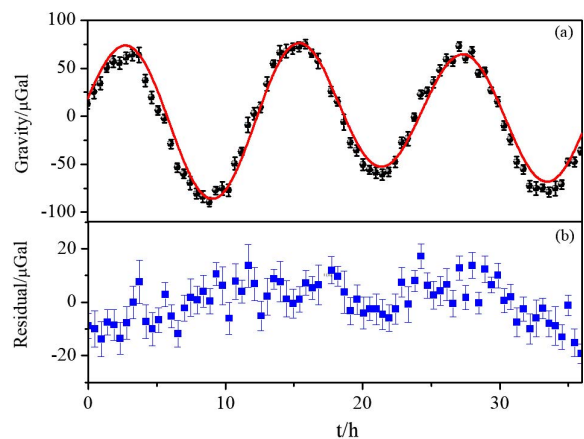


Fig. 4. Tidal data measured by our CCAG. (a) is the experimental data and tidal model, where black scatters represent measured gravity value and the red line represents tidal model. (b) shows the residual between them.

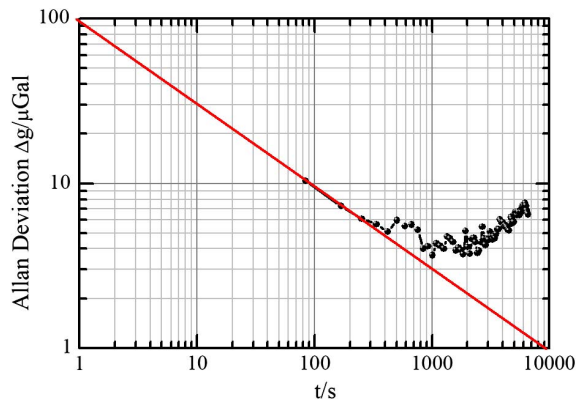


Fig. 5. Allan deviation of the residual.



Fig. 6. Truck for the transportation of our CCAG.

In Beijing, the absolute gravity value at three test sites was measured, and each site took about 12 h to continuously measure the data. Figure 7 shows the test field in Beijing.

Before carrying out the gravity measurement, the tilt adjustment of the vacuum chamber should be done such that the big gravity offset caused by misalignment can



Fig. 7. Atom gravimeter runs normally in the test site. The test sites are well-isolated from vibration, and the temperature and humidity in the test room are well controlled.

be avoided. A tilt meter is fixed solidly to monitor the tilt drift of the Raman retro-reflector mirror. The tilt meter could record the tilt of the vacuum chamber in two dimensions, named as tilt x and tilt y , respectively. The experimental data could be fitted by a parabolic function so that the tilt point insensitive to gravity could be obtained, and the results are shown in Fig. 8. After, the values are stored by an acquisition card and are corrected to the measured gravity value. We record the real-time tilt values of the sensor and then compensate the deviation caused by them when dealing with the gravity data, which makes it possible to recover measurements after moving from one site to another quickly.

With respect to the instrument corrections and uncertainties, we acquired an instrument correction of $-157.5 \mu\text{Gal}$ and an uncertainty of $19.0 \mu\text{Gal}$ in this comparison, as shown in Table 1, which includes the frequency reference, two-photon light shift, laser frequency bandwidth, and so on. Some corrections, such as wavefront aberrations of Raman beams and the Coriolis effect, were not evaluated in this comparison, but we evaluate these deviations in our laboratory after that.

The final corrected gravities of each site are displayed in Fig. 9. The red scatters are the reference values given by the NIM. It can be seen that our measured values are of

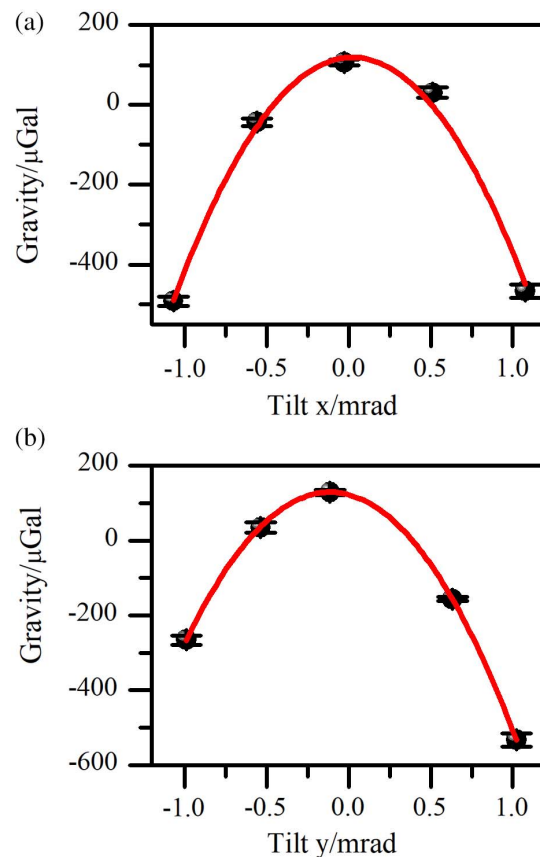


Fig. 8. The adjustment of the tilt before carrying out the absolute gravity measurement.

Table 1. The Budget for the Evaluation of Measurement Uncertainty

Influence Parameters	Corrections/ μGal	Uncertainties/ μGal
Frequency reference	-82.0	2.0
Two-photon light shift	-64.0	10.0
Laser frequency reproducibility	0.0	15.0
Laser frequency bandwidth	0.0	6.0
Direction of two reversed Raman lasers	0.0	1.0
Measurement height corrections	-11.5	0.1
Total uncertainty	-157.5	19.0

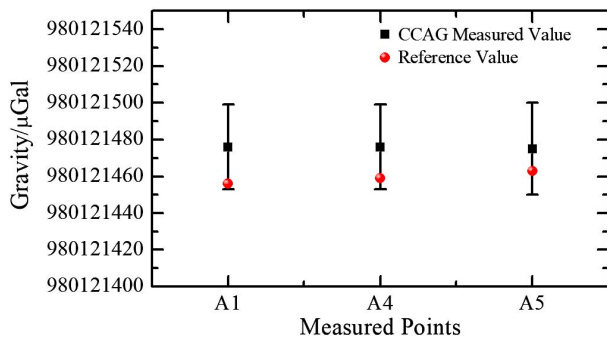


Fig. 9. The comparison between our results and the given reference value.

good consistence with the reference values. The reference value is the weighted average value of several participating high-precision AGs, such as FG5 and FG5X. It is given by the NIM.

In conclusion, we have already accomplished a CCAG with a portable and stable laser system. The laser system is based on two DFB laser diodes with the wavelength of 1560 nm. The gravity sensitivity of $90 \mu\text{Gal}/\sqrt{\text{Hz}}$ has been achieved. Moreover, a continuous gravity monitoring of 36 h is carried out.

Then, a CCAG was transported about 1200 km to Beijing to participate in the APMP.M.G-K1 comparison. The gravity values of three sites were measured as requested by the organizer. The accuracy budget is formulated by considering the significant terms, such as Raman laser frequency uncertainty, two-photon light shift, and more, with the total instrument uncertainty of $19 \mu\text{Gal}$.

The successful participation in the international gravity measurement campaign has proven the mobility and robustness of our system. The sensitivity of our cold atom gravimeter is comparable with the commercial FG5. The accuracy of the instrument needs more study and further improvement.

This work was supported by the National Key Research and Development Program of China (Nos. 2017YFC0601602 and 2016YFF0200206) and the National Natural Science Foundation of China (Nos. 61727821, 61475139, 11604296, and 11174249).

References

1. M. P. Poland and D. Carbone, *J. Geophys. Res.-Sol. Ea.* **121**, 5477 (2016).
2. S. Okubo, Y. Tanaka, S. Ueki, H. Oshima, T. Maekawa, and Y. Imanishi, *Earth Planets Space* **65**, 563 (2013).
3. B. Fores, C. Champollion, N. Le Moigne, R. Bayer, and J. Chery, *Geophys. J. Int.* **208**, 269 (2017).
4. S. Merlet, Q. Bodart, N. Malossi, A. Landragin, F. P. Dos Santos, O. Gitlein, and L. Timmen, *Metrologia* **47**, L9 (2010).
5. C. Freier, M. Hauth, V. Schkolnik, B. Leykauf, M. Schilling, H. Wziontek, H. G. Scherneck, J. Muller, and A. Peters, *J. Phys. Conf. Ser.* **723**, 012050 (2016).
6. A. Louchet-Chauvet, S. Merlet, Q. Bodart, A. Landragin, F. P. Dos Santos, H. Baumann, G. D'Agostino, and C. Origlia, *IEEE Trans. Instrum. Meas.* **60**, 2527 (2011).
7. O. Francis and H. Baumann, *Metrologia* **49**, 07014 (2012).
8. O. Francis, H. Baumann, T. Volarik, C. Rothleitner, G. Klein, M. Seil, N. Dando, R. Tracey, C. Ullrich, S. Castelein, H. Hu, K. Wu, C. Y. Shen, S. B. Xuan, H. B. Tan, Z. Y. Li, V. Palinkas, J. Kostecky, J. Makinen, J. Naranen, S. Merlet, T. Farah, C. Guerlin, F. P. Dos Santos, N. Le Moigne, C. Champollion, S. Deville, L. Timmen, R. Falk, H. Wilmes, D. Iacovone, F. Baccaro, A. Germak, E. Biolcati, J. Krynski, M. Sekowski, T. Olszak, A. Pachuta, J. Agren, A. Engfeldt, R. Reudink, P. Inacio, D. McLaughlin, G. Shannon, M. Eckl, T. Wilkins, D. van Westrum, and R. Billson, *Metrologia* **50**, 257 (2013).
9. D. Schmerge, O. Francis, J. Henton, D. Ingles, D. Jones, J. Kennedy, K. Krauterbluth, J. Liard, D. Newell, R. Sands, A. Schiel, J. Silliker, and D. van Westrum, *J. Geodesy* **86**, 591 (2012).
10. Z. Jiang, V. Palinkas, F. E. Arias, J. Liard, S. Merlet, H. Wilmes, L. Vitushkin, L. Robertsson, L. Tisserand, F. P. Dos Santos, Q. Bodart, R. Falk, H. Baumann, S. Mizushima, J. Makinen, M. Bilker-Koivula, C. Lee, I. M. Choi, B. Karaboce, W. Ji, Q. Wu, D. Ruess, C. Ullrich, J. Kostecky, D. Schmerge, M. Eckl, L. Timmen, N. Le Moigne, R. Bayer, T. Olszak, J. Agren, C. Del Negro, F. Greco, M. Diamant, S. Deroussi, S. Bonvalot, J. Krynski, M. Sekowski, H. Hu, L. J. Wang, S. Svitlov, A. Germak, O. Francis, M. Becker, D. Inglis, and I. Robinson, *Metrologia* **49**, 666 (2012).
11. O. Francis, H. Baumann, C. Ullrich, S. Castelein, M. Van Camp, M. A. de Sousa, R. L. Melhorato, C. J. Li, J. Y. Xu, D. W. Su, S. Q. Wu, H. Hu, K. Wu, G. Li, Z. Li, W. C. Hsieh, P. V. Palinkas, J. Kostecky, J. Makinen, J. Naranen, S. Merlet, F. P. Dos Santos, P. Gillot, J. Hinderer, J. D. Bernard, N. Le Moigne, B. Fores, O. Gitlein, M. Schilling, R. Falk, H. Wilmes, A. Germak, E. Biolcati, C. Origlia, D. Iacovone, F. Baccaro, S. Mizushima, R. De Plaen, G. Klein, M. Seil, R. Radinovic, M. Sekowski, P. Dykowski, I. M. Choi, M. S. Kim, A. Borreguero, S. Sainz-Maza, M. Calvo, A. Engfeldt, J. Agren, R. Reudink, M. Eckl, D. van Westrum, R. Billson, and B. Ellis, *Metrologia* **52**, 07009 (2015).
12. S. K. Wang, Y. Zhao, W. Zhuang, T. C. Li, S. Q. Wu, J. Y. Feng, and C. J. Li, *Metrologia* **55**, 360 (2018).
13. T. M. Niebauer, G. S. Sasagawa, J. E. Faller, R. Hilt, and F. Klopping, *Metrologia* **32**, 159 (1995).
14. S. Okubo, S. Yoshida, T. Sato, Y. Tamura, and Y. Imanishi, *Geophys. Res. Lett.* **24**, 489 (1997).
15. J. Le Gouet, T. E. Mehlstaubler, J. Kim, S. Merlet, A. Clairon, A. Landragin, and F. P. Dos Santos, *Appl. Phys. B* **92**, 133 (2008).

16. M. Kasevich and S. Chu, *Phys. Rev. Lett.* **67**, 181 (1991).
17. F. Riehle, T. Kisters, A. Witte, J. Helmcke, and C. J. Borde, *Phys. Rev. Lett.* **67**, 177 (1991).
18. Y. N. Wang, Y. L. Meng, J. Y. Wan, L. Xiao, M. Y. Yu, X. Wang, X. C. Ouyang, H. D. Cheng, and L. Liu, *Chin. Opt. Lett.* **16**, 070201 (2018).
19. X. S. Yan, C. F. Wu, J. Q. Huang, J. W. Zhang, and L. J. Wang, *Chin. Opt. Lett.* **15**, 040202 (2017).
20. G. Lamporesi, A. Bertoldi, L. Cacciapuoti, M. Prevedelli, and G. M. Tino, *Phys. Rev. Lett.* **100**, 050801 (2008).
21. P. Clade, E. de Mirandes, M. Cadoret, S. Guellati-Khelifa, C. Schwob, F. Nez, L. Julien, and F. Biraben, *Phys. Rev. Lett.* **96**, 033001 (2006).
22. J. B. Fixler, G. T. Foster, J. M. McGuirk, and M. A. Kasevich, *Science* **315**, 74 (2007).
23. S. Dimopoulos, P. W. Graham, J. M. Hogan, and M. A. Kasevich, *Phys. Rev. Lett.* **98**, 111102 (2007).
24. S. Fray, C. A. Diez, T. W. Hansch, and M. Weitz, *Phys. Rev. Lett.* **93**, 240404 (2004).
25. S. Dimopoulos, P. W. Graham, J. M. Hogan, M. A. Kasevich, and S. Rajendran, *Phys. Lett. B* **678**, 37 (2009).
26. L. Zhou, S. T. Long, B. Tang, X. Chen, F. Gao, W. C. Peng, W. T. Duan, J. Q. Zhong, Z. Y. Xiong, J. Wang, Y. Z. Zhang, and M. S. Zhan, *Phys. Rev. Lett.* **115**, 013004 (2015).
27. Z. K. Hu, B. L. Sun, X. C. Duan, M. K. Zhou, L. L. Chen, S. Zhan, Q. Z. Zhang, and J. Luo, *Phys. Rev. A* **88**, 043610 (2013).
28. P. Gillot, O. Francis, A. Landragin, F. P. Dos Santos, and S. Merlet, *Metrologia* **51**, L15 (2014).
29. Q. Y. Wang, Z. Y. Wang, Z. J. Fu, W. Y. Liu, and Q. Lin, *Opt. Commun.* **358**, 82 (2016).
30. S. Merlet, L. Volodimer, M. Lours, and F. P. Dos Santos, *Appl. Phys. B* **117**, 749 (2014).
31. B. Fang, I. Dutta, P. Gillot, D. Savoie, J. Lautier, B. Cheng, C. L. G. Alzar, R. Geiger, S. Merlet, F. P. Dos Santos, and A. Landragin, *J. Phys. Conf. Ser.* **723**, 012049 (2016).
32. M. Hauth, C. Freier, V. Schkolnik, A. Senger, M. Schmidt, and A. Peters, *Appl. Phys. B* **113**, 49 (2013).
33. Y. Bidet, O. Carraz, R. Charriere, M. Cadoret, N. Zahzam, and A. Bresson, *Appl. Phys. Lett.* **102**, 144107 (2013).
34. A. Peters, K. Y. Chung, and S. Chu, *Metrologia* **38**, 25 (2001).